evolutionary fabrication emerged as a consequence of the idea of embodiment.

The pivotal realization is that *buildability* is a central concept in generative robotics. There is little meaning in the ability to produce design blueprints if these cannot be executed/self-reproduced.

"Approaching Fully Automated Design and Manufacture from this perspective requires a new formulation of Evolutionary Design, one that replaces descriptive blueprints with prescriptive assembly plans. In this approach, the formation of an object can no longer be taken for granted; we must realistically simulate not only the behavior of a finished object, but its entire assembly as well" (Rieffel 2006).

This is what Rieffel refers to as the *fabrication gap:* by merely specifying the form of an object, this approach leaves unanswered the vital question of formation. Rieffel's concept revolves around the idea of *situated development*. The assembly process is a part of the evaluation criteria of the fitness function for the evolutionary design process; how cleverly a structure is built is part of the evaluation criteria while the structure is being optimized. Evolutionary computing is used not only to arrive at a global optimum of a design given a set of constraints, but also, in this approach, to simultaneously generate an optimized assembly plan. Figure 8 demonstrates the potential of Rieffel's coupled approach; here the objective of the design is to maximize the shading area. The poetic term ontogenic scaffolding refers to the temporary elements used while assembling the structure. The dynamics of the assembly are simulated and subvert the assembly constraints. As a result, integrating and exploiting the assembly constraints bring about an interesting notion: where the unfinished structure is effectively used as a tool, raising the idea of self-referential fabrication; where the construction of a structure implies this unfinished structure as an essential means of production until it is completed, when it progressively ceases to be a tool. Nadine Sterk's lamp design Sleeping Beauty suggests such an approach. Can a pavilion be a tool for the production of that pavilion until it is completed and effectively stops being a tool? An approach developed by the Cornell Creative Machines Lab research on robotically manipulatable structures (Lobo, Hjelle, and Lipson 2009) moves toward such procedures, where robots continuously disassemble and reassemble a constant number of structural elements to facilitate an ever-changing architectural program, an approach inspired by metabolism.

Evolutionary fabrication holds great architectural potential. Both the design and building processes are simultaneously optimized, which inspires the realization that—much the way the evolution of a robot's body requires the evolution of its brain—exploiting the true capacity of robotics in architecture requires the simultaneous evolution of building and construction processes.

REFERENCES

Bergin, T. J., Jr., and R. G. Gibson, Jr., eds. (1996). History of Programming Languages—II. New York, NY: ACM.

Frazer, J. (1995). An Evolutionary Architecture. London: Architectural Association Publications.

Funes, P., and J. Pollack. (1998). Evolutionary Body Building: Adaptive Physical Designs for Robots. Artificial Life 4: 337–57.

Kelly, K. (2010). What Technology Wants. New York: Viking Adult.

Lobo, D., D. A. Hjelle, and H. Lipson. (2009). Reconfiguration Algorithms for Robotically Manipulatable Structures. In ASME/IFToMM International Conference on Reconfigurable Mechanisms and Robots, ReMAR 2009, 13–22.

Minhat, M., V. Vyatkin, X. Xu, S. Wong, and Z. Al-Bayaa. (2009). A Novel Open CNC Architecture Based on Step-NC Data Model and IEC 61499 Function Blocks. Robotics and Computer-Integrated Manufacturing 25(3): 560–69.

Morel, P. (2010). The Linguistic Turn of Architectural Production.

Null, C., and B. Caulfield. (2003). Fade to Black: The 1980s Vision of "Lights-Out" Manufacturing, Where Robots Do All the Work, Is a Dream No More. Business 2.0 (June 1). http://money.cnn.com/magazines/business2/business2_archive/2003/06/01/343371/index.htm.

Rieffel, J. (2006). Evolutionary Fabrication: The Co-Evolution of Form and Formation. PhD thesis, Brandeis University, Waltham, MA.

Ross, D. T. (1978). Origins of the Apt Language for Automatically Programmed Tools. SIGPLAN Notices 13(8): 61–99.

SIGGRAPH. (2011). Bridging Synthetic and Organic Materiality: Graded Transitions in Material Connections. In ACM SIGGRAPH 2011 Studio Talks, SIGGRAPH '11, 10:1. New York, NY: ACM.

Spiekermann, E. (1995). LettError. http://letterror.com.

Werfel, J. (2006). Anthills Built to Order: Automating Construction with Artificial Swarms. PhD thesis, Massachusetts Institute of Technology, Cambridge, MA. AAI0810111.

THE FORBIDDEN SYMMETRIES

Rima Ajlouni
Texas Tech University

ABSTRACT

The emergence of quasiperiodic tiling theories in mathematics and material science is revealing a new class of symmetry that has never been accessible before. Due to their astounding visual and structural properties, quasiperiodic symmetries can be ideally suited for many applications in art and architecture, providing a rich source of geometry for exploring new forms, patterns, surfaces, and structures. However, since their discovery, the unique long-range order of quasiperiodic symmetries is still posing a perplexing puzzle. As rule-based systems, the ability to algorithmically generate these complicated symmetries can be instrumental in understanding and manipulating their geometry.

Recently, the discovery of quasiperiodic patterns in ancient Islamic architecture is providing a unique example of how ancient mathematics can inform our understanding of some basic theories in modern science. The latest investigations into these complex and chaotic formations is providing evidence to show that ancient designers, by using the most primitive tools (a compass and a straightedge), were able to resolve the complicated long-range principles of tenfold quasiperiodic formations.

Derived from these ancient principles, this paper presents a computational model to describe the long-range order of octagon-based quasiperiodic formations. The objective of the study is to design an algorithm for constructing large patches of octagon-based quasiperiodic formations. The proposed algorithm has proven to be successful in producing an infinite and defect-free covering of the two-dimensional plane.

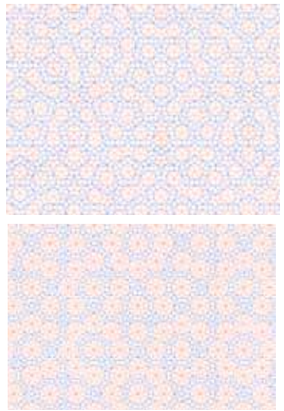

figure 1

1 INTRODUCTION

While the use of mathematics in art and architecture has historically denoted principles of order, balance, proportion, symmetry, and perfect form, contemporary mathematical theories, supported by computer power, have recently emerged as a new paradigm for design creativity and innovation, in which design is being engaged in a broader sphere, oscillating between different disciplines (i.e., architecture, art, engineering, mathematics, computer science, material science, biology, etc.). In this multidisciplinary sphere, contemporary mathematical theories, including fractals, inflation-deflation, scale-invariance, self-similarity, and complex hierarchies, are being embraced as a rich source of stimulus for articulating new patterns, forms, surfaces, structures, and materials.

The emergence of quasicrystalline tiling theories in mathematics and material science is revealing an exciting new class of symmetry that has never been explored before. The interest in these mysterious symmetries was triggered mainly by the discovery of quasicrystals in 1984 (Shechtman et al. 1984). This new state of matter exhibits ***f****orbidden symmetries*, which were thought to be impossible for the crystalline matter in classical crystallography. The atoms in these complicated structures are not arranged according to regularly spaced intervals, similar to traditional crystals; instead, they exhibit a complicated long-range translational order that is not periodic (Levine and Steinhardt 1986; Yamamoto and Takakura 2008). Since their first discovery, the number and variety of quasicrystals has become quite extensive; however, the unique long-range signature of quasicrystalline (quasiperiodic) symmetries still poses a perplexing puzzle (Boissieu, Currat, and Francoual 2008; Ishii and Fujiwara 2008).

Today, the race to unlock the global mathematical mystery of quasicrystalline geometry is highly competitive. Understanding these new symmetries can help provide a deeper understanding of the structure of quasicrystals at an atomic scale, allowing scientists to achieve improved control over their composition and structure, potentially leading to the development of new materials and devices (Mikhael et al. 2008; Dubois 2002; Tsai and Gomez 2008). Moreover, because of their astounding visual and structural properties, quasiperiodic symmetries can be ideally suited for many applications in art and design (Robbin 1996), providing a whole new class of geometry that has never been accessible before.

The recent discovery of ancient ornaments with similar quasiperiodic symmetries is providing a new insight into understanding the global order of these complicated formations. By using a compass and a straightedge, ancient designers were able to resolve the complicated long-range principles of tenfold quasiperiodic formations. Derived from the same principles, this paper presents a computational model, based on a compass and straightedge algorithm, to describe the global long-range order of eightfold quasiperiodic symmetries.

2 LITERATURE REVIEW

In their attempt to resolve the quasicrystalline symmetries, scientists turned to studying abstract structure models, which are based on tiling of space. Only a limited number of tiling models exist for describing quasicrystals. The most famous ones were described by Penrose and Ammann-Beenker. The Penrose pentagonal tilings discovered by mathematical physicist Roger Penrose in the 1970s (Penrose 1974) consist of two differently shaped tiles that join according to local matching rules (Figure 1a). The Ammann-Beenker octagonal tiling (Figure 1b) consists of two pieces, a square and a diamond, constructed based on local matching rules (Grünbaum and Shephard 1986).

Since the discovery of quasicrystals, these tiling patterns are still used as the main template for studying the structure of quasicrystals. Mathematically, quasiperiodic tilings can be generated using the matching rules (Penrose 1974; Grünbaum and Shephard 1986), the inflation–deflation method (De Bruijn 1981a), the grid method (De Bruijn 1981b), the strip projection method (Kramer 1982), the cut projection method (Bak 1986), and the generalized dual method (Socolar et al. 1985). Whereas significant progress has been made in determining their local order, the mathematical principles of the *global long-range quasiperiodic order* remain an open question (Boissieu, Currat, and Francoual 2008; Ishii and Fujiwara 2008).

figure 1

(a) Penrose pentagonal tiling pattern. (b) Ammann-Beenker octagonal tiling.

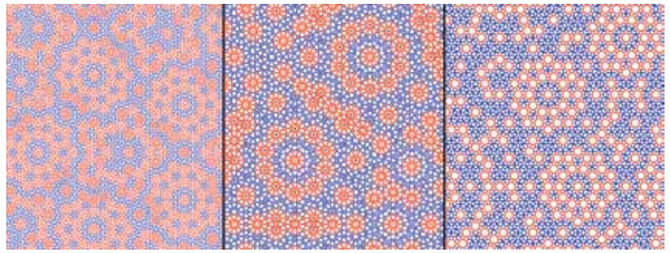

figure 2

2.1 Islamic Quasiperiodic Patterns

Recently, the discovery of ancient ornaments in Islamic architecture with similar quasicrystalline symmetries has triggered significant investigations into understanding their mathematical laws and generating principles (Makovicky 1992; Makovicky et al. 1998; Bonner 2003; Lu and Steinhardt 2007; Makovicky 2008; Makovicky and Makovicky 2011). Astonishingly, eight centuries before their discovery in modern times, ancient artists had constructed patterns with perfect tenfold quasicrystalline formations (Al Ajlouni 2012). Examples of these patterns can be found on the external walls of Gunbad-I Kabud tomb tower in Maragha, Iran (1197 C.E) (Figure 2a), the walls of the Madrasa of al-'Attarin (1323 CE) in Fez, Morocco (Figure 2b), and the walls of Darb-i Imam shrine and the Friday Mosque in Isfahan, Iran (1453 CE) (Figure 2c). These patterns offer a rich data source that can be of great benefit to many scientific fields, including arts, architecture, mathematics, theoretical physics, crystallography, chemistry, biology, etc. (Kritchlow 1976; Abas and Salman 1992; El-Said 1993; Kaplan 2000; Al Ajlouni 2009, 2011, 2012).

The latest investigation into these complex and chaotic formations reveals a deeper connection between contemporary theories and traditional mathematics. Compelling evidence suggests that ancient designers made a conceptual breakthrough in mathematics as early as the 12th century by constructing complex geometry far more mathematically advanced than we ever thought possible. By using basic tools (a compass and a straightedge) ancient designers were able to resolve the complicated long-range principles of quasiperiodic formations (Al Ajlouni 2012). Derived from these principles, Al Ajlouni (2012) proposed the first global multilevel hierarchical framework model (HFM) to describe the long-range translational and orientational order of fivefold and tenfold quasiperiodic formations. This model provides the only available global long-range structural method that is able to construct infinite patches of perfect fivefold and tenfold quasicrystalline formations, including Penrose tilings, without the need for confusing tiling strategies or complicated mathematics (Al Ajlouni 2011). The proposed hierarchical framework, which presents a philosophical shift in construction principles, provides important clues to understanding the global generating principles of other types of quasiperiodic symmetries.

3 RESEARCH DESIGN

3.1 Research Hypothesis

The use of simple consecutive geometry (based on a compass and straightedge method) provides important clues to understanding the global generating principles of tenfold quasiperiodic patterns. By adopting the same hierarchical organizational principles, it is possible to develop computational models for describing the long-range order of other types of nonperiodic geometry. Derived from the same ancient mathematical principles, this paper investigates the use of similar hierarchical frameworks to construct the global empire of octagon-based quasicrystalline formations.

figure 2

a) The quasicrystalline empire of the pattern on the external walls of Gunbad-I Kabud tomb tower in Maragha, Iran (1197 CE). (b) The quasicrystalline empire of the pattern on the walls of the Madrasa of al-'Attarin (1323 CE) in Fez, Morocco. (c) The quasicrystalline empire of the pattern on the walls of Darb-i Imam shrine and the Friday Mosque in Isfahan (1453 CE) in Isfahan, Iran.

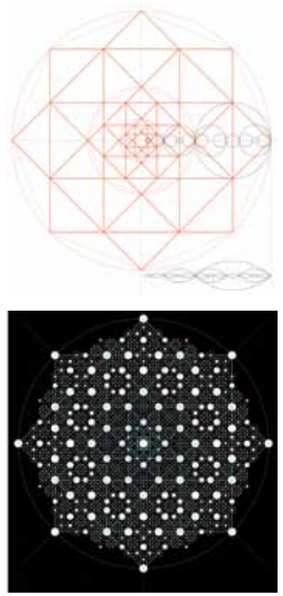

figure 3

figure 3

A framework of a sequence of nested octagrams. (a) The progression of nested decagrams grows based on the sequence. (b) The geometrical correlation between the framework of nested octagrams and X-ray diffraction pattern of octagonal quasicrystal formations.

The research follows an empirical paradigm in developing its algorithm and uses experimentation as its main strategy. Both quantitative and qualitative approaches were used in developing the algorithm and evaluating its performance.

3.2 Target Population

For the purpose of conducting this study, algorithms specifically target the octagonal quasiperiodic tiling of Ammann–Beenker, with the assumption that it provides a true representative sample of all octagon-based quasiperiodic populations. Although this research focuses specifically on octagonal tiling, the underlying goal is to develop general ideas and principles that might be applied to other types of quasiperiodic symmetries.

In the following description, an algorithm is presented to construct the global empire of octagon-based quasicrystalline symmetries, producing an infinite and defect-free covering of the two-dimensional plane.

3.3 Instrumentation

The computer algorithm was designed in C++ language and performed using computers supporting OpenGL and the OpenGL interface API GLUT. The free C++ compiler and development environment Bloodshed Dev-C++ was used for Windows operating systems.

4 ALGORITHMS DESIGN

The process of constructing the global empire of the Ammann-Beenker tiling pattern is demonstrated in the following four sections: the Underlying Basic Grid, the First Hierarchy, the Second Hierarchy, and the Infinite Empire.

4.1 The Underlying Basic Grid

The proposed algorithm conforms to the ancient method of construction by a simple compass and straightedge method in which the generating force of patterns lies in the center of the circle. It is derived from the principle that patterns are based on a combination of an underlying basic grid and repeating units (Al Ajlouni 2012). While the basic grid is used to define the type of symmetry by defining the positions of repeating units within the overall formation, the design of the repeating units defines the internal variations of the patterns' design, without affecting the overall symmetry. Accordingly, the underlying basic grid is the key to resolving the long-range order of octagon-based quasiperiodic symmetries.

According to the proposed algorithm, the arrangements of all repeating units within the global empire are determined based on one global framework. A framework of nested octagrams (Figure 3a) serves as the underlying basic grid. A strong geometrical correlation exists between the framework of nested octagrams and X-ray diffraction pattern of octagonal quasicrystal formations. This correlation (Figure 3b) is demonstrated by overlapping the framework of nested octagrams with a diffraction pattern of octagonal quasicrystals. As shown in Figure 3b, according to their intensity level, these diffraction peaks are organized in a hierarchical fashion that works in perfect concert with the sequence of the nested octagrams. The framework grows based on the sequence. If we denote the radius of the nth octagram by radn and the next larger radius by radn+1, then the ratio radn+1/radn is equal to .

Equation 1 $\mathrm{n}_0 \rightarrow \mathrm{n}_\infty, \quad \frac{rad_{n+1}}{rad_n} = \sqrt{2}+1$

The mathematical growth of the nested octagrams (Figure 4) and all the intersection points within the framework are governed by equations 2, 3, and 4.

Equation 2 $\frac{rad_1}{rad_0} = \frac{rad_2}{rad_1} = \frac{rad_3}{rad_2} = \frac{rad_{n+1}}{rad_n} \quad \sqrt{2}+1$

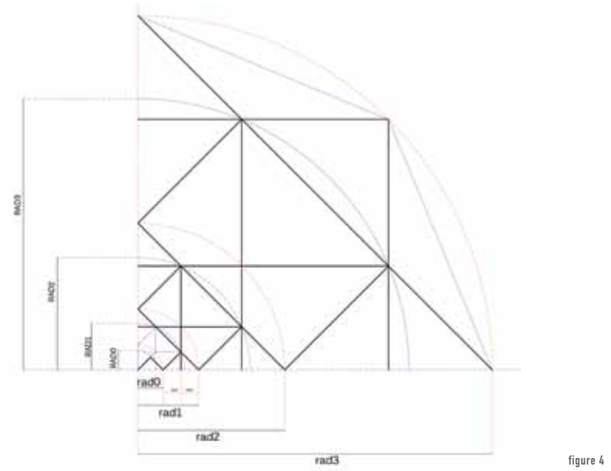

figure 4

figure 4

The mathematical growth of the nested octagrams.

Equation 3 $\mathrm{n}_0 \rightarrow \mathrm{n}_\infty, \quad \frac{\mathrm{RAD}_{n+1}}{\mathrm{RAD}_n} = \sqrt{2}+1$

Equation 4 $\mathrm{RAD}_{n+1} = \sqrt{\left(\mathrm{rad}_n + \frac{\mathrm{rad}_{n+1}+\mathrm{rad}_n}{2}\right)^2 + \left(\frac{\mathrm{rad}_{n+1}+\mathrm{rad}_n}{2}\right)^2}$

Similarly, the proposed algorithm is based on a multilevel hierarchical order. In this order, the global empire is constructed of infinite levels of hierarchical clusters. Any cluster level, in this hierarchy, is composed of two smaller building clusters: one highly symmetrical seed cluster and one fragment. In the following section, the construction of the first-hierarchy cluster is demonstrated for Ammann–Beenker tiles.

4.2 The First Hierarchy

The quasiperiodic empire is generated around one main *center of origin:* the center of the global eightfold proportional system. Figure 5a demonstrates the process of constructing the central repeating unit. The size and design of the central star *seed* unit is proportional to the size of the framework and is strictly derived from the diminution sequence of the nested octagrams (Figure 5c). If we denote the radius of the *seed* unit by radn and the radius of the first hierarchy framework by radn+2, then the ratio radn+2/radn is equal to = 5.828427 .

Equation 5 $\frac{\mathrm{rad}_{n+2}}{\mathrm{rad}_n} = 2\sqrt{2}+3$

The positions of all *seed* units are determined entirely by the network of the nested octagrams. The black dots in figure 5c correspond to the center position of all instances of the *seed* unit (Figure 5d). The connecting formations between the main *seed* units are determined by arrangements of smaller blue octagons (Figure 5d). The octagon's internal design is actually a fragment of the main seed unit (Figure 5b). The final quasiperiodic pattern of the first hierarchy is shown in Figure 5e.

The algorithm for constructing the main seed unit is shown in Appendix 1. The algorithm for constructing the fragment-connecting unit is shown in Appendix 2. All intersection points within the framework are calculated based on equations 2 and 4. The relative size of the seed unit, as it related to the framework, is calculated based on equation 5. The final locations of the main seed units are calculated based on equations 2 and 4. The algorithm for calculating the final pattern of the first hierarchy is shown in Appendix 3.

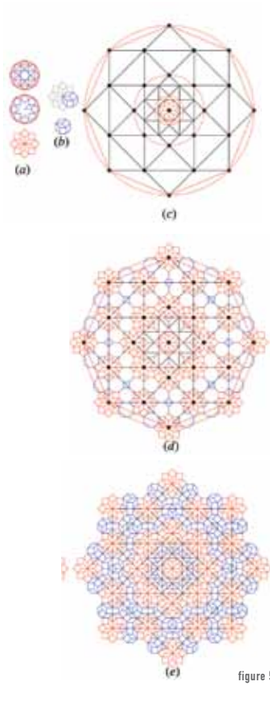

figure 5

figure 5

The sequence of constructing the first-level hierarchy of Ammann-Beenker quasiperiodic tiling. (a) The construction process of the main seed unit. (b) The construction process of the fragment unit. (c) The framework of the nested octagrams. (d) The distribution of all seed units within the framework. (e) The final quasiperiodic pattern of the first hierarchy.

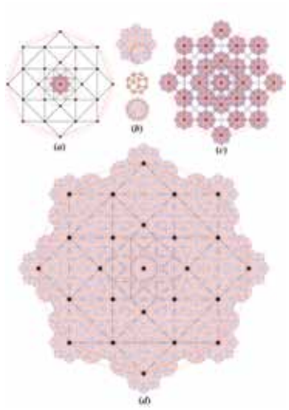

figure 6

figure 6

The sequence of constructing the second-level hierarchy of Ammann-Beenker quasiperiodic tiling patterns. (a) A new generation of the framework of the nested octagrams. (b) The main repeating seed cluster and the fragment cluster. (c) The distribution of all seed clusters within the framework. (d) The final quasiperiodic pattern of the second hierarchy.

4.3 The Second Hierarchy

The construction process of the second-level hierarchy is similar to the process of constructing the first-level order, explained earlier. The only difference is that the *seed* unit in the second-level hierarchy is actually the final constructed cluster pattern of the first-level hierarchy (Figure 5e). These *seed* clusters are distributed according to a new generation of nested decagrams (Figure 6a). The relative ratio of the new larger framework as it related to the seed cluster is equal to and is calculated based on *equation* 5. The black dots in Figure 6a correspond to the center position of all instances of the *seed* cluster (Figure 6c). The final locations of the main seed clusters are calculated based on *equations* 2 and 4. The connecting formations between the main seed clusters are determined by arrangements of the smaller blue octagons (Figure 6c). The internal arrangement of the connecting octagon is derived from the design of the main cluster (Figure 6b). The final quasiperiodic formation of the second hierarchy empire is shown in Figure 6d.

4.4 The Infinite Empire

The construction of the infinite empire of the octagon-based quasiperiodic pattern requires building a progression of multilevel hierarchical formations. In this infinite multigeneration order, the geometric arrangement of the next higher-level order is governed by a new generation of the nested octagrams, which is derived from the proportional system. In this sequence, the final generated pattern of the previous order (Figure 6d) acts as the *seed* cluster of the new generation-order. This process can grow indefinitely to build an infinite structure of octagon-based quasicrystal formations.

5 CONCLUSIONS

In conclusion, a computational mathematical model is presented for constructing the global empire of quasiperiodic Ammann–Beenker tiling. The suggested model shows that cluster configurations and the geometric arrangements of the multigeneration clusters are determined entirely by a geometric progression of the nested octagrams. It also shows that the position of building units, locally and globally, is defined by one global framework, and not based on local rules.

The proposed algorithm is successful in describing the long-range order of Ammann–Beenker tiling, providing an easy tool for architects, mathematicians, physicists, teachers, designers, and artists to generate and implement these complicated quasiperiodic formations. The conceptual framework proposed by this study can serve as a platform for developing professional software related to quasiperiodic symmetries.

Future efforts should be directed toward investigating the application of similar hierarchal global models to generate other types of quasiperiodic formations, including sevenfold, ninefold, twelve-fold, and sixteenfold quasiperiodic symmetries.

REFERENCES

Abas, S. J., and A. Salman. (1992). Geometric and Group-Theoretic Methods for Computer Graphic Studies of Islamic Symmetric Patterns. Computer Graphics Forum 11(1): 43–53.

Al Ajlouni, R. (2009). Digital Pattern Recognition in Heritage Recording: An Automated Tool for Documentation and Reconstruction of Visually Complicated Geometric Patterns. Germany: Verlag-DM.

Al Ajlouni, R. (2011). A Long-Range Hierarchical Clustering Model for Constructing Perfect Quasicrystalline Formations. Philosophical Magazine 91: 2728–38.

Al Ajlouni, R. (2012). The Global Long-Range Order of Quasiperiodic Patterns in Islamic Architecture. Acta Crystallographica A68: 235–43.

Bak, P. (1986). Icosahedral Crystals: Where Are the Atoms? Physical Review Letters 56: 861–64.

Boissieu, M., R. Currat, and S. Francoual. (2008). Phason Modes in Aperiodic Crystals. In Quasicrystals, eds. T. Fujiwara and Y. Ishii, 107–62. Amsterdam: Elsevier.

Bonner, J. (2003). Three Traditions of Self-Similarity in Fourteenth and Fifteenth Century Islamic Geometric Ornament. In Proceedings of ISAMA/Bridges: Mathematical Connections in Art, Music and Science, eds. R. Sarhangi and N. Friedman, 1–12. Spain: University of Granada.

De Bruijn, N. G. (1981b). Algebraic Theory of Penrose's Non-periodic Tilings of the Plane. Proc. Math. 43: 53–66.

De Bruijn, N. G., (1981a). Sequences of Zeros and Ones Generated by Special Production Rules. Proc. Math. 43: 27–37.

Dubois, J. (2002). Bulk and Surface Properties of Quasicrystalline Materials and Their Potential Applications. In Quasicrystals: An Introduction to Structure, Physical Properties, and Applications, Vol. 55, eds. J. B. Suck, M. Schreiber, and P. Haussler, 507–32. Berlin: Springer-Verlag.

El-Said, E. (1993). Islamic Art and Architecture: The System of Geometric Design. 1st ed. Reading, England: Garnet Publishing Ltd.

Gahler, F., and H. Jeong. (1995). Quasiperiodic Ground States Without Matching Rules. Phys. A: Math. Gen 28: 1807–15.

Grünbaum, B., and G. C. Shephard (1986). Tilings and Patterns. New York: Freeman.

Ishii, Y., and T. Fujiwara. (2008). Electronic Structures and Stability of Quasicrystals. In Quasicrystals, eds. T. Fujiwara and Y. Ishii, 171–203. Amsterdam: Elsevier.

Kaplan, C. (2000). Computer Generated Islamic Star Patterns. Bridges 2000, Mathematical Connections in Art, Music and Science. Waterloo, Ontario: UW School of Computer Science. Accessed March 15, 2004. http://www.cgl.uwaterloo.ca.

Kramer, P. (1982). Non-periodic Central Space Filling with Icosahedral Symmetry Using Copies of Seven Elementary Cells. Acta Crystallographica 38: 257–64.

Kritchlow, K. (1976). Islamic Patterns: An Analytical and Cosmological Approach. New York: Thames & Hudson, Inc.

Levine, D., and P. Steinhardt. (1986). Quasicrystals. 1. Definition and Structure. Physical Review B 34: 596–616.

Lu, P., and P. Steinhardt. (2007). Decagonal and Quasicrystalline Tilings in Medieval Islamic Architecture. Science 315: 1106–10.

Makovicky, E. (1992). Fivefold Symmetry, ed. I. Hargittai, 67–86. Singapore: World Scientific.

Makovicky, E. (2008). Symmetry Culture. Sci. 19: 127–51.

Makovicky, E., and N. Makovicky. (2011). The First Find of Dodecagonal Quasiperiodic Tiling in Historical Islamic Architecture. Journal of Applied Crystallography 44: 569–73.

Makovicky, E. and P. Fenoll Hach-Alı´. (1996). Mirador de Lindaraja: Islamic Ornamental Patterns Based on Quasiperiodic Octagonal Lattices in Alhambra, Granada, and Alcazar, Sevilla, Spain. Bol. Soc. Esp. Mineral. 19: 1–26.

Mikhael, J., J. Roth, L. Helden, and C. Bechinger. (2008). Archimedean-like Tiling on Decagonal Quasicrystalline Surfaces. Nature 454: 501–04.

Penrose, R. (1974). The Role of Aesthetics in Pure and Applied Mathematical Research. Bulletin of the Institute of Mathematics and Its Applications 10: 266–71.

Robbin, T. (1996). Engineering a New Architecture. New Haven and London: Yale University Press.

Shechtman, D., I. Blech, D. Gratias, and J. W. Cahn. (1984). Metallic Phase with Long-Range Orientational Order and No Translational Symmetry. Physical Review Letters 53: 1951–53.

Socolar, J., P. Steinhardt, and D. Levine. (1985). Quasicrystals with Arbitrary Orientational Symmetry. Physical Review B 32: 5547–50.

Tsai, A., and C. P. Gomez. (2008). Quasicrystals and Approximants in Cd–M Systems and Related Alloys. In Quasicrystals, eds. T. Fujiwara and Y. Ishii, 75–104. Amsterdam: Elsevier.

Yamamoto, A., and H. Takakura. (2008). Recent Development of Quasicrystallography. In Quasicrystals, eds. T. Fujiwara and Y. Ishii, 11–47. Amsterdam: Elsevier.

APPENDIX 1

```
#define   PI               3.1415926536    /* mathematical Pi (constant) */
#define CIRC_INC_2         (2 * PI / 8)    /* for Octagon */

//Draw the Star "seed" unit with center at position (x, y), radius rad and Red, green,
blue and alpha values
void STAR_UNIT(float xc, float yc, float rad, float RCV, float GCV, float BCV, float ACV)
  {
    float theta, dis1, dis2, rad1, x1, y1, x2, y2, x3, y3, x4, y4, x5, y5;
    dis1= rad/ (1+ sqrt (2));
    dis2=(rad-dis1)/2;
    rad1= sqrt ((dis1+dis2)*(dis1+dis2)+ (dis2 *dis2) );

    for(theta=0.0; theta < 2 * PI; theta += CIRC_INC_2)
         {
         x1= (xc+rad*cos(theta)); y1= (yc+rad*sin(theta));
         x2= (xc+rad1*cos(theta-PI/8)); y2= (yc+rad1*sin(theta-PI/8));
         x3= (xc+dis1*cos(theta));y3= (yc+dis1*sin(theta));
         x4= (xc+rad1*cos(theta+PI/8)); y4= (yc+rad1*sin(theta+PI/8));
         x5= (xc+dis1*cos(theta +PI/4 )); y5= (yc+dis1*sin(theta +PI/4));

  //Draw the square tile
  glColor4f(RCV, GCV, BCV, ACV );
  glBegin(GL_LINE_LOOP);
    glVertex2f(x1,y1); glVertex2f(x2,y2); glVertex2f(x3,y3); glVertex2f(x4,y4);glVertex2f
(x1,y1);
  glEnd();
  //Draw the diamond tile
  glBegin(GL_LINE_LOOP);
    glVertex2f(xc,yc);  glVertex2f(x3,y3); glVertex2f(x4,y4); glVertex2f(x5,y5);
  glEnd();
  //Draw points at the intersections
glColor4f(1.0, 1.0, 1.0,1.0 );
glBegin(GL_POINTS);
    glVertex2f(xc,yc); glVertex2f(x1,y1); glVertex2f(x2,y2); glVertex2f(x3,y3);glVertex2f
(x4,y4);
glEnd();
         }
  }
```


APPENDIX 2

```
/*Draw the fragment unit with position (x, y), radius rad, Red, green, blue and alpha
values, and theta*/
void FRAGMENT(float xc, float yc, float rad, float RCV, float GCV, float BCV, float ACV,
float theta)
  {
  float dis1, dis2, rad1, rad1_1, x1, y1, x2, y2, x3, y3, x4, y4, x5, y5, x6, y6, x7, y7,
x8, y8, x9, y9, x10, y10;
  dis1= rad/ (1+ sqrt (2));
  dis2=(rad-dis1)/2;
  rad1= sqrt ((dis1+dis2)*(dis1+dis2)+ (dis2 *dis2) );
  rad1_1 = sqrt ((dis1*dis1)+ (rad *rad) );

     x1= (xc+rad*cos(theta-PI/8)); y1= (yc+rad*sin(theta-PI/8));
     x2= (xc+rad1*cos(theta-PI/4)); y2= (yc+rad1*sin(theta-PI/4));
     x3= (xc+dis1*cos(theta-PI/8));  y3= (yc+dis1*sin(theta-PI/8));
     x4= (xc+rad1*cos(theta)); y4= (yc+rad1*sin(theta));
     x5= (xc+dis1*cos(theta +PI/8) );y5= (yc+dis1*sin(theta +PI/8) );
     x6= (xc+dis1*cos(theta -3*(PI/8) ));y6= (yc+dis1*sin(theta -3*(PI/8) ));
     x7= (xc+rad1_1*cos(theta)); y7=(yc+rad1_1*sin(theta));
     x8= (xc+rad*cos(theta+PI/8 )); y8=(yc+rad*sin(theta+PI/8 ));
     x9= (xc+rad1*cos(theta+(PI/4) ));y9=(yc+rad1*sin(theta+(PI/4) ));
     x10=(xc+dis1*cos(theta+(3*PI/8) )); y10=(yc+dis1*sin(theta+(3*PI/8) ));

   glColor4f(RCV, GCV, BCV, ACV );
   glBegin(GL_LINE_LOOP);
       glVertex2f(x1,y1);glVertex2f(x2,y2);glVertex2f(x3,y3);glVertex2f(x4,y4);
   glEnd();

   glBegin(GL_LINE_LOOP);
       glVertex2f(xc,yc);glVertex2f(x3,y3);glVertex2f(x2,y2);glVertex2f(x6,y6);
   glEnd();

   glBegin(GL_LINE_LOOP);
       glVertex2f(xc,yc);glVertex2f(x3,y3);glVertex2f(x4,y4);glVertex2f(x5,y5);
   glEnd();

   glBegin(GL_LINE_LOOP);
       glVertex2f(xc,yc);glVertex2f(x5,y5);glVertex2f(x9,y9);glVertex2f(x10,y10);
   glEnd();

   glBegin(GL_LINE_LOOP);
       glVertex2f(x1,y1);glVertex2f(x7,y7);glVertex2f(x8,y8);glVertex2f(x4,y4);
   glEnd();

   glBegin(GL_LINE_LOOP);
       glVertex2f(x4,y4);glVertex2f(x5,y5);glVertex2f(x9,y9);glVertex2f(x8,y8);
   glEnd();

   glColor4f(1.0, 1.0, 1.0,1.0 );
   glBegin(GL_POINTS);
       glVertex2f(xc,yc);glVertex2f(x1,y1;glVertex2f(x2,y2);glVertex2f(x3,y3);
       glVertex2f(x4,y4);glVertex2f(x5,y5);glVertex2f(x6,y6);glVertex2f(x7,y7);
       glVertex2f(x8,y8);glVertex2f(x9,y9);glVertex2f(x10,y10);
   glEnd();
}
```

APPENDIX 3

```
/*Draw the first hierarchy pattern center at position (x, y) and radius rad */
void FIRST_HIERARCHY(float x, float y, float rad)
      {
float dis1, dis2, rad1, rad1_1, theta, rad2, rad3, rad4,rad5, DIS_1, DIS_2;
  dis1= rad/ (1+ sqrt (2));
  dis2=(rad-dis1)/2;
  rad1= sqrt ((dis1+dis2)*(dis1+dis2)+ (dis2 *dis2) );
  rad1_1 = sqrt ((dis1*dis1)+ (rad *rad) );
  rad2= rad *(1+ sqrt (2));
  rad3= rad2 *(1+ sqrt (2));
  DIS_1= rad2;
  DIS_2=(rad3-rad2)/2;
  rad4= sqrt ((DIS_1+DIS_2)*(DIS_1+DIS_2)+(DIS_2 *DIS_2) );
   // Draw Framework and the central seed unit
  STAR_UNIT (x, y, rad, 0.0, 1.0, 0.0, 1.0);
  STAR_UNIT (x, y, rad2, 1.0, 0.0, 0.0, 1.0);
  STAR_UNIT (x, y, rad3, 1.0, 0.0, 0.0, 1.0);
  //Draw the star units according to the framework
  glBegin(GL_LINE_LOOP);
    for(theta=0.0; theta < 2 * PI; theta += CIRC_INC_2)
      {STAR_UNIT (x+rad2*cos(theta),y+rad2*sin(theta), rad, 0.0, 1.0, 0.0, 1.0);}
  glEnd();
  glBegin(GL_LINE_LOOP);
    for(theta=0.0; theta < 2 * PI; theta += CIRC_INC_2)
      {STAR_UNIT (x+rad3*cos(theta),y+rad3*sin(theta), rad, 0.0, 1.0, 0.0, 1.0);}
  glEnd();
  glBegin(GL_LINE_LOOP);
    for(theta=0.0; theta < 2 * PI; theta += CIRC_INC_2)
      {STAR_UNIT (x+rad4*cos(theta+PI/8),y+rad4*sin(theta+PI/8),rad, 0.0, 1.0, 0.0,
1.0);}
  glEnd();
  // Draw the connecting fragments
  for(theta=PI/8; theta < 2 * PI; theta += PI/4)
     {
     FRAGMENT(x+(rad1+ rad1_1)*cos(theta),y+(rad1+ rad1_1)*sin(theta),
              rad, 0.0, 0.0,1.0, 1.0, theta + PI);
     FRAGMENT(x+(2*rad1+ rad1_1)*cos(theta),y+(2*rad1+ rad1_1)*sin(theta),
               rad, 0.0, 0.0,1.0, 1.0, theta);
     }
for(theta=PI/4; theta < 2 * PI; theta += PI/4)
    {
     FRAGMENT(x+(rad2+ rad)*cos(theta),y+(rad2+ rad)*sin(theta),
              rad, 0.0, 0.0,1.0, 1.0, theta-(3*PI/8));
     FRAGMENT(x+(rad2+ rad)*cos(theta),y+(rad2+ rad)*sin(theta),
              rad, 0.0, 0.0,1.0, 1.0, theta+(3*PI/8));
     FRAGMENT(x+(rad2+ rad)*cos(theta)+(rad)*cos(theta + PI/4),
              y+(rad2+ rad)*sin(theta)+(rad)*sin(theta+ PI/4),
              rad, 0.0, 0.0,1.0, 1.0, theta-(PI/8));
     FRAGMENT(x+(rad2+ rad)*cos(theta)+(rad)*cos(theta - PI/4),
              y+(rad2+ rad)*sin(theta)+(rad)*sin(theta- PI/4),
              rad, 0.0, 0.0,1.0, 1.0, theta+(PI/8));
    }
for(theta=PI/8; theta < 2 * PI; theta += PI/4)
    {
     FRAGMENT(x+(rad4)*cos(theta)+(rad)*cos(theta + PI/8),
              y+(rad4)*sin(theta)+(rad)*sin(theta+ PI/8),
              rad, 0.0, 0.0,1.0, 1.0, theta+(PI/2));
     FRAGMENT(x+(rad4)*cos(theta)+(rad)*cos(theta - PI/8),
              y+(rad4)*sin(theta)+(rad)*sin(theta- PI/8),
              rad, 0.0, 0.0,1.0, 1.0, theta-(PI/2));
    }
  }
```


WORK IN PROGRESS

AN EXPLORATION INTO COMPUTATIONAL OPTIMIZATION FOR MOTIVE ARCHITECTURE

ABSTRACT

This paper explores the potential of advanced computational methods for kinetic architecture. An experiment has been conducted with the aim of applying a genetic algorithm on the walking behavior of a physical prototype. The choice of the scissor mechanism is arbitrary; this is to convey that the adaptive behavior of a structure may be improved in real time with the appropriate computational methods, regardless of its mechanical complexity. This provides architects with the opportunity to bring previously static architectural concepts into motion. This work looks to the fields of embodied artificial intelligence (AI) and mobile robotics research as resources for integrating evolutionary computation into physical artifacts.

Ryan Mehanna
MSc Adaptive Architecture
and Computation

The Bartlett School of Graduate Studies
University College London

Elite Sher
MSc Adaptive Architecture
and Computation

The Bartlett School of Graduate Studies
University College London